Geophys. J. Int. (2006) **166,** 126–134 doi: 10.1111/j.1365-246X.2006.02936.x

Motional induction voltage measurements in estuarine environments: the Ria de Aveiro Lagoon (Portugal)

Rita Nolasco,[1] António Soares,[1] João M. Dias,[2] Fernando A. Monteiro Santos,[1,3] N. A. Palshin,[4] Patricia Represas[1] and Nuno Vaz[2]

[1]*Centro de Geofísica da Universidade de Lisboa, Campo Grande,* C8, 1749-016 *Lisboa, Portugal. E-mail: rnolasco@sapo.pt*
[2]*Departamento de Física, Universidade Aveiro,* 3810-193 *Aveiro, Portugal*
[3]*Departamento de Física da Universidade de Lisboa, Campo Grande,* C8, 1749-016 *Lisboa, Portugal*
[4]*Shirshov Institute of Oceanology, Moscow, Russia*

Accepted 2006 January 23. Received 2005 October 18; in original form 2004 September 21

SUMMARY

Electromagnetic fluctuations in the ocean have external sources like ionospheric–magnetospheric current systems, and purely internal oceanic sources associated with interaction between water velocity fields and the geomagnetic field, that is, the motionally induced voltage (MIV). During the last decade techniques based on MIV have proven to provide reliable information when applied to the flow monitoring at large oceanic channels. In this paper analysis of data resulting from the implementation of these techniques in a small-scale system, that is, the Ria de Aveiro lagoon (Portugal), is presented.

A submarine cable crossing the channel at the entrance of the lagoon (Barra channel) allows the measurement of the potential difference between two electrodes located on both sides of the channel. Spectral analysis of these data reveals that measured voltages are dominated by semidiurnal M_2, S_2/K_2 frequencies. Comparison between the sum of the four main constituents determined by harmonic analysis and the sea surface elevation measured at a tide gauge located at the lagoon mouth reveal that the measured potential difference is proportional to the water flow. To estimate the water flow in this location from the MIV measurements the data collected using this methodology were compared with numerical results obtained from a previously calibrated hydrodynamic model. A value of 720 $m^3\ s^{-1}\ mV^{-1}$ was estimated for the coefficient relating voltage and water transport at Barra. Taking this value into account a sediment layer of about 20 m is estimated, at Barra.

The results show that it is possible to indirectly measure the water transport (by tidal and residual flows) through the channel by measuring the differences of electrical potential. This demonstrates the applicability of the MIV method to a small-scale system.

Key words: electromagnetic, motionally induced electric field, submarine cables, tides.

1 INTRODUCTION

The electrical potential difference between a pair of electrodes placed in a channel, perpendicularly to the water flow, depends basically on, (i) the telluric field (electric), generated by the variations of the geomagnetic field, (ii) the water flow and the electric properties of the fluid and iii) the electric structure of the terrain underlying the channel (e.g. Sanford 1971). The recording of the variation of the electrical potential difference between the electrodes, with an adequate sampling rate and over a long recording period yield a measure of the variations of the mass transport with time, and hence, its seasonal and even interannual variations.

Oceanographers interest in the motionally induced electric field as a tool to study ocean flow and to provide information about the velocity structure of ocean currents is increasing. The method of towed dipoles and the use of submarine cables are two examples of electromagnetic approaches to measure oceanic flows (e.g. Filloux 1987; Chave *et al.* 1992; Palshin *et al.* 1999).

Most experience with submersed electrodes connected by submarine cables have been carried out at large scale (hundred to thousands km), for example between California and Hawaii (Chave *et al.* 1992); to study the Florida current (Larsen 1992; Flosadottir & Taire 1997); in the Sea of Japan (Palshin *et al.* 2001); between Madeira and Sesimbra (Monteiro Santos *et al.* 2002). Some small-scale (1–10 km) experiments were carried out, for example, in the Strait of Magellan (Harvey *et al.* 1977), at the Throat of the White Sea (Palshin *et al.* 2002) and in Oresund connection between the Baltic and the Kattegat-Skagerrak (Fristedt *et al.* 2002).

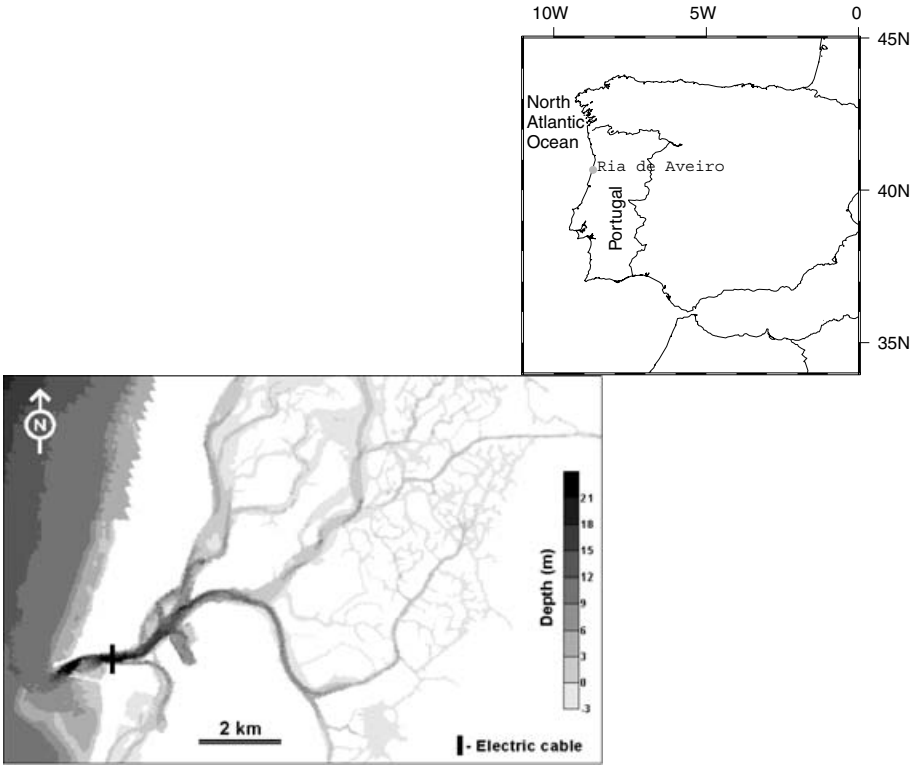

Figure 1. Location of the cable at the Ria de Aveiro lagoon.

This work presents the results obtained by applying the motionally induced voltage (MIV) method to a small scale (about 1/2 km) estuarine system where tidal currents are important.

It is nowadays recognized that coastal and estuarine environments are significant locations for bio-diversity evolution. Because of their nature, biota are extremely sensitive to changes in the boundary conditions, particularly in those, which concern water properties. This perception has triggered a large research activity in order to understand the parameters controlling the dynamics of those systems. Therefore, the development of analytical tools and their validation with real time data is clearly important to model the behaviour of such environments. Significant physical parameters that need to be monitored are the water flow into the ecosystem, the water temperature distribution and the water salinity.

The Ria de Aveiro is an example of this kind of system. It is a shallow water lagoon with a very complex geometry, connected with the Atlantic Ocean through a single artificial channel, the Barra channel of 300 m width and from 3 to 25 m depth (Fig. 1). All of its water exchange with the ocean takes place by input/output across this narrow entrance. The current velocity varies from 0 to 3 m s^{-1} with typical values of about 1–1.5 m s^{-1} (Dias *et al.* 2003). The input of fresh water comes from several small rivers distributed by different channels of the lagoon. The most important river (the Vouga river) is responsible for approximately two-thirds of the fresh water input into the lagoon (Dias *et al.* 1999). These characteristics make Ria de Aveiro an ideal place to implement and test innovative sensing systems dedicated to monitoring estuaries and coastal zones.

A system composed of two silver-silver-chloride (Ag/AgCl) nonpolarizable electrodes, connected to a voltmeter by submarine cables, was installed at the entrance of the lagoon, the Barra channel, to allow the estimation of the water transport/flow at this site. The electrodes were specially designed for sea applications and the distance between them is 280 m.

The electrical potential difference between the two electrodes was measured using a 16-bit datalogger. The sampling rate of the datalogger is 10 s, but only the average of six values over 60 s is recorded.

The electrical potential difference measurements started on 2002 July 23, and have continued until the time of writing.

This paper deals with the analysis of data acquired between 2002 July 23 and November 13. Its main objective is to test the possibility of using the MIV method at Ria de Aveiro and to calculate the transport calibration coefficient of the measurement system. The data analysis reveals an accurate estimate of the water transport (by tidal and residual flows) through Barra channel from the differences of electrical potential measured across the channel.

2 SEPARATION OF MOTIONALLY INDUCED SIGNAL

Fig. 2(a) shows the electric potential difference recorded between 2002 July 23 and November 13, across the channel at Barra. The potential difference varies between about −13 and 13 mV. Hourly means have been computed to suppress outliers in the time-series. A comparison between minutely and hourly means data allows to verify how efficient this method is (Fig. 2b).

The most important experimental detail affecting the accuracy of long-term voltage measurements, the bias voltage ($\Delta\phi_N$), is the stability of the cable-ocean contacts. The voltage difference between a pair of similar electrodes in sea water is mainly a function of the temperature and salinity. The voltage difference for the usually small temperature and salinity differences in the ocean can be approximated by the linear relation (Larsen 1992):

$$\Delta\phi_N \approx \beta_T(T_1 - T_2) + \beta_S(S_1 - S_2), \quad (1)$$

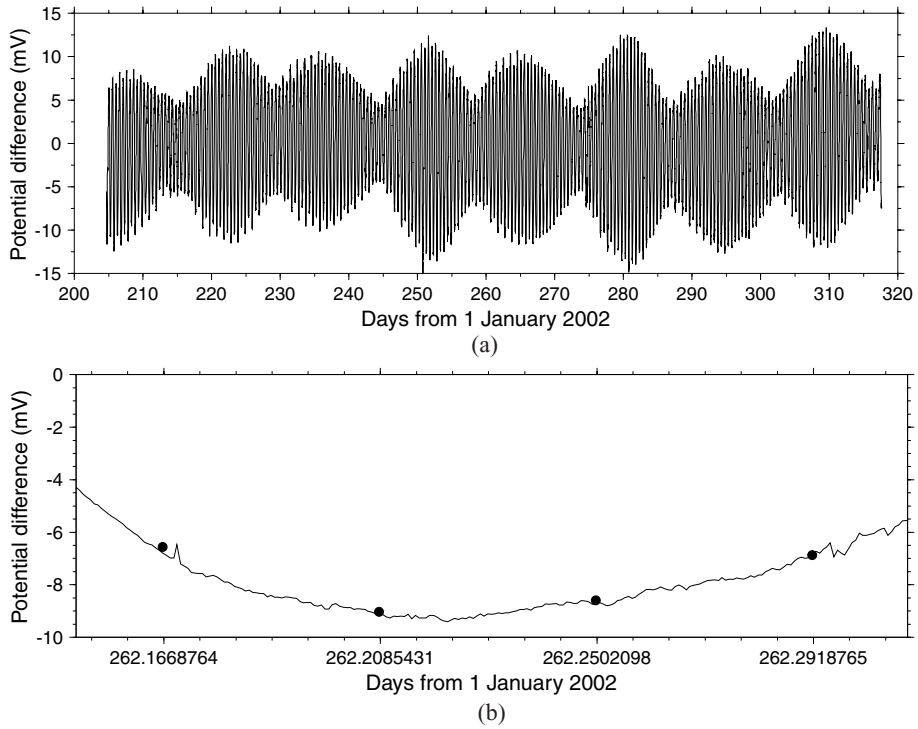

Figure 2. (a) Hourly means of the potential difference across the lagoon in Barra, measured between two electrodes located on both sides of the lagoon. Records obtained between 2002 July 23 and November 13. (b) A typical 4-hr-long section of minutely (line) data and hourly means (solid symbols).

where T and S are, respectively, the temperature and salinity at electrodes 1 and 2 and β_T and β_S are, respectively, the temperature and salinity coefficients for a pair of electrodes.

Silver-silver-chloride electrodes are a class of electrodes called reference electrodes where the metal is in equilibrium with a saturated solution of a slightly soluble salt. The coefficients for electrodes in sea water were approximated experimentally (Larsen 1992) by:

$$\beta_T \approx 0.517 \text{ mV } ^\circ\text{C}^{-1} \quad \text{and} \quad \beta_S \approx -1.145 \text{ mV ppt}^{-1}. \tag{2}$$

The ranges of temperature and salinity (see Fig. 3) at the location of the electrodes are compatible with those estimated by Larsen with similar silver-silver-chloride electrodes.

Temperature and salinity measurements at or close to the electrodes do not exist for the recording period of this experiment. However, data are available at the same location as the cable, close (about 5 m) to the electrodes, between 2003 September 26 and 2004 September 22, (Fig. 3a) providing an order of magnitude estimate of $\Delta\phi_N$ in the electric potential difference registers. The sampling rate was approximate twice per month, at neap and spring tide, just after low tide while water level is increasing. The bias voltage, given by eqs (1) and (2), due to temperature and salinity difference between the electrodes is plotted in Fig. 3(b).

The temperature and salinity induced voltage variation is lower than 1 mV for this period of time. These values (lower than 1 mV) during the recording period, give rise to a bias voltage of less than 7 per cent of the observed $\pm$13 mV signal. Although this is a relatively high value it cannot be the source of electric potential difference drift, since this bias voltage fluctuates in time. In fact there is no drift in the results shown in Fig. 2. On the other hand this bias can not be directly related to flood or ebb flow, because the measurements are taken always at flood, and the signal of $\Delta\phi_N$ changes in time.

The amplitude spectrum of the hourly mean electrical potential differences is plotted in Fig. 4.

The spectrum of the measured voltages (Fig.4) is dominated by semidiurnal M_2, S_2/K_2 frequencies. P_1/K_1, O_1 and M_4 frequencies are also present, with smaller amplitudes. The M_2 constituent amplitude is higher than the S_2/K_2 or any other frequency in the spectrum. This means that the tidal, M_2, induced electric field is stronger than other constituents of the electric field. The time-series also provides the visualization of the spring-neap tidal cycle and the diurnal-inequality characteristic of mixed tidal regime (Fig. 2).

The constituents M_2, N_2, O_1 and M_4 are mainly of oceanic tidal motional origin. The constituents S_2/K_2 and P_1/K_1 are a combination of oceanic tidal motion and geomagnetic origin. The main objectives of this study are (1) to verify whether the MIV technique, usually applied at large-scale studies, can be used at our shorter scale and (2) to estimate the calibration coefficient between MIV and the water transport using the lunar constituents of tides, as mentioned before. Therefore, this study will focus on the four (M_2, N_2, O_1, M_4) constituents of lunar origin.

The measured time-series was approximated by a set of lunar harmonic constituents using least square fitting (LSF) method (Pawlowicz *et al.* 2002). The results of LSF are presented in Fig. 5 where Fig. 5(a) shows the four lunar constituents with 95 per cent confidence interval and Fig. 5(b) shows the sum of these four constituents (from now on this sum will be named MIV_L). Fig. 5(c) presents the residual time-series calculated as the difference between recorded data and MIV_L.

There is a tide gauge located at the southern side of the channel, 10 m away from the southernmost electrode. The available sea surface elevation (SSE) data were digitized, using a sample rate of 1 hr. These data are displayed in Fig. 6(a).

The SSE harmonic constituents of lunar origin (M_2, N_2, O_1 and M_4) were also obtained using a least square fitting method (Pawlowicz *et al.* 2002). The same processing procedure used for the electric potential difference was applied to SSE data. Fig. 6(b)

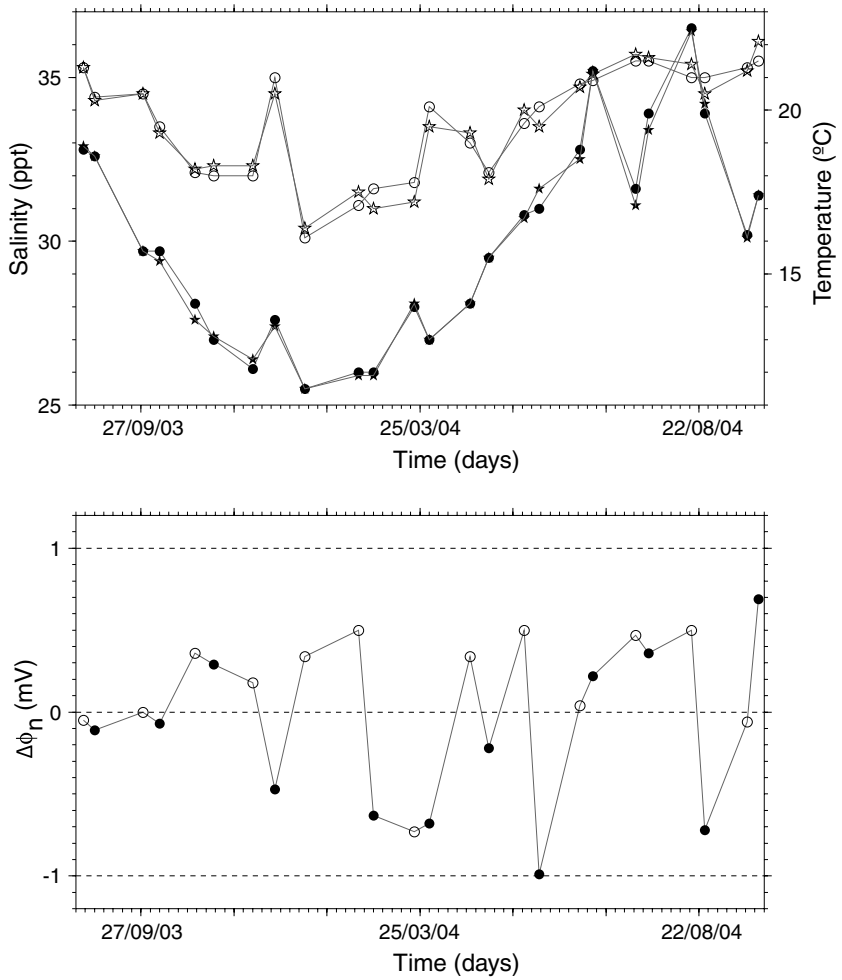

Figure 3. (a) Temperature (solid symbols) and salinity (open symbols) recorded close (about 5 m) to the electrodes, (electrode north denoted by circles and electrode south denoted by stars). Records obtained between 2003 September 26 and 2004 September 22. (b) Bias voltage induced by the temperature and salinity difference between electrode north and south. The bias voltage are obtained through measurements taken near the time of spring tide (open symbols) and near neap tide (solid symbols).

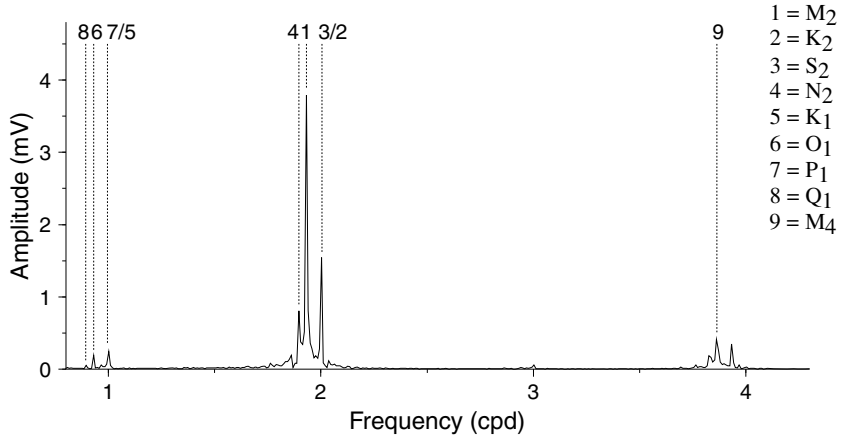

Figure 4. Amplitude spectrum obtained from electrical potential difference data recorded between 2002 July 23 and November 13.

shows the sum of the constituents with lunar origin MIV_L (dashed line) and the equivalent sum resulting from SSE (solid line). A difference of 0.088 days between the maximum values of electric potential difference and SSE (sums of the lunar constituents) can be noted.

The propagation of the tide in a shallow system such as the Ria de Aveiro represents a balance between the inertia of the water mass, the pressure force due to the slope of the water surface, and the retarding force resulting from bottom friction. The momentum of the water mass causes the current to continue to flow against an

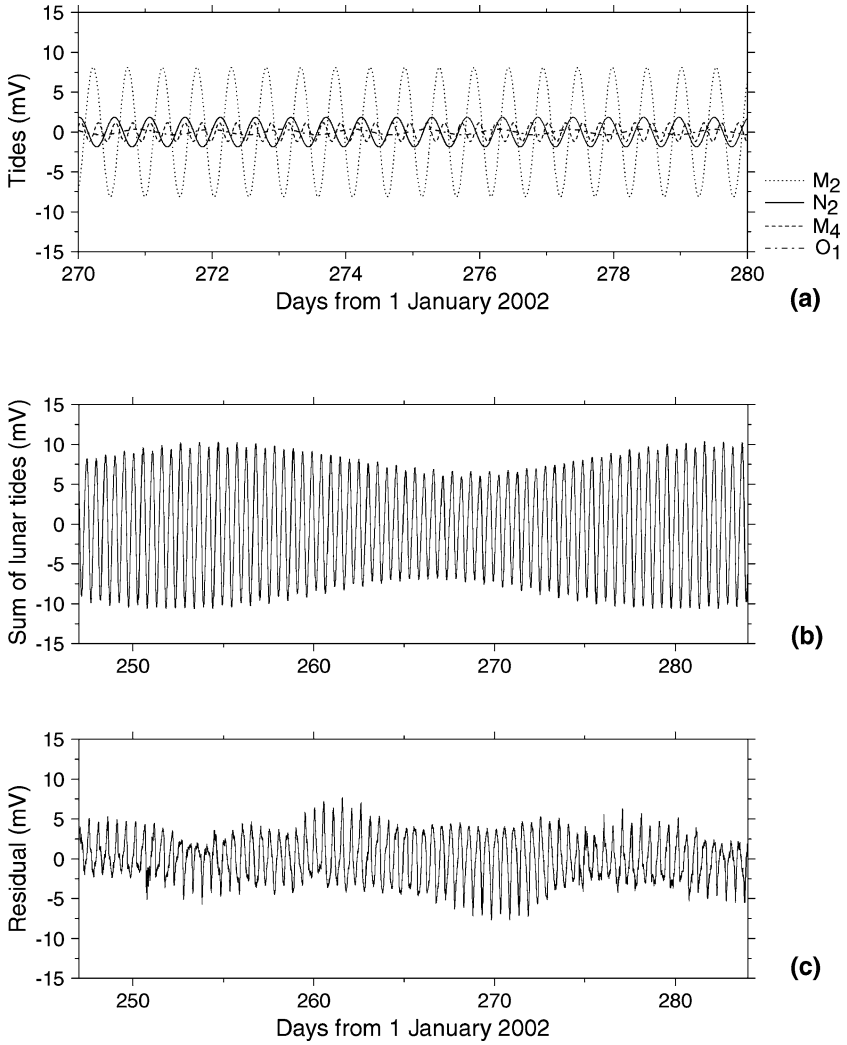

Figure 5. Results of least-square analysis of the average potential difference collected between 2002 July 23 and November 13. (a) The selected four constituents with lunar origin. (b) Sum of the four constituents designed in this paper as MIV_L (c) Residual time-series obtained after removing the MIV_L presented in (b).

opposing pressure gradient and therefore a phase shift is expected between the water flux and the SSE (Dias 2001). In fact Dias (2001) analysed the delay of the local current inversion relative to high and low water at the lagoon mouth, for both neap and spring tide conditions, based on numerical modelling results. It is observed that tidal elevations and velocities are usually not in phase and that high water occurs before high slack tide and low water before low slack tide. The values found are not the same for the high water and the low water cases, ranging from about 70 min (high water of neap tide) to about 120 min (low water of spring tide). Therefore, the phase shift determined in this work (0.088 days or about 127 min) is consistent with the numerical results and may be explained as follows, assuming that the MIV_L is proportional to the water flux.

3 DISCUSSION (CALIBRATION OF MIV USING NUMERICAL MODEL)

In the absence of water fluxes measurements at the mouth of the lagoon in the Barra-Atlantic Ocean channel, results from a hydrodynamic numerical model (Dias 2001; Dias & Lopes in press) were used to determine the calibration factor between motional field and water transport.

Considering the characteristics of the Ria de Aveiro a 2-D vertically integrated hydrodynamic model was considered to be an appropriate choice to simulate this lagoon hydrodynamics (Dias 2001). This model was developed from the SIMSYS2D code (Leendertse & Gritton 1971; Leendertse 1987), which solves the shallow water equations:

$$\frac{\partial \varsigma}{\partial t} + \frac{\partial (HU)}{\partial x} + \frac{\partial (HV)}{\partial y} = 0, \tag{3}$$

$$\frac{\partial U}{\partial t} + U\frac{\partial U}{\partial x} + V\frac{\partial U}{\partial y} = fV - g\frac{\partial \varsigma}{\partial x} + \frac{\tau_x^s - \tau_x^b}{H\rho} + A_h \nabla^2 U, \tag{4}$$

$$\frac{\partial V}{\partial t} + U\frac{\partial V}{\partial x} + V\frac{\partial V}{\partial y} = -fU - g\frac{\partial \varsigma}{\partial y} + \frac{\tau_y^s - \tau_y^b}{H\rho} + A_h \nabla^2 V, \tag{5}$$

where U and V are the depth integrated velocity components in the x (eastward) and y (northward) directions, respectively, ς is the surface water elevation, H is the water height, t is the time, f is the Coriolis parameter, g is the acceleration of gravity, ρ is the water density, A_h is the kinematical turbulent horizontal viscosity, τ^s and τ^b are, respectively, the magnitude of the wind stress on the water surface and the magnitude of the bottom shear.

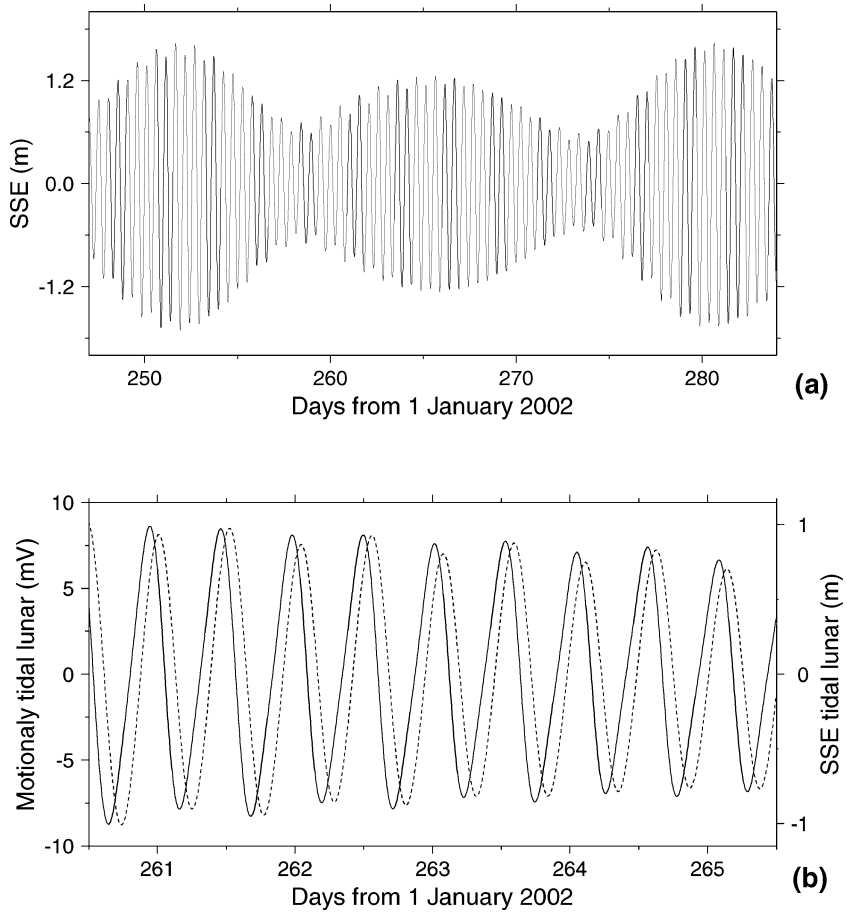

Figure 6. (a) Sea surface elevation (SSE) measured at the tide gauge. (b) MIV_L in solid line, and the resulting of the sum of the significant harmonics of the SSE in dashed line. The time lag between the two series is about 0.088 days.

The system of eqs (3)–(5) was discretized using a finite difference method and the difference equations solved by the ADI (alternating direction implicit) method, using a space-staggered grid (Leendertse & Gritton 1971; Dias 2001).

With appropriate boundary and initial conditions, this system of equations constitutes a well-posed problem whose solution describes the depth-averaged circulation in a tidal basin, and allows the determination of the SSE, current velocity and water fluxes in any area of the computational domain.

The numerical bathymetry is specified within a box of size $\Delta x = \Delta y = 100$ m, resulting in 160 cells in the x direction and 393 cells in the y direction. At the ocean open boundary the water elevation over the reference level was imposed using SSE data measured at the Barra tide gauge.

This model was properly calibrated for Ria de Aveiro lagoon through comparison between model results and measurements of SSE and current velocity, for several stations distributed along the main lagoon channels. This calibration is described in earlier publications (Dias 2001; Dias & Lopes 2006).

The water transport time-series computed by the numerical model for the transversal section corresponding to the cable location (Fig. 1) and the water transport amplitude spectrum are displayed in Figs 7(a) and (b), respectively.

As expected, different tidal constituents, with oceanic moon and sun origin and respective combinations, are identified in the water transport spectrum. As mentioned before, only the electric potential difference induced by the lunar constituents (M_2, N_2, O_1 and M_4) will be compared with the modelled water transport. In order to obtain the water transport with tidal lunar (M_2, N_2, O_1 and M_4) origin, the model time- series was approximated by a set of lunar harmonics using the statistical least square fitting (LSF) method (Pawlowicz *et al.* 2002). Again the same data processing procedure used regarding the electric potential difference and the SSE data was used. The results are shown in Fig. 8.

Fig. 9 shows the relation between the sum of the four oceanic constituents of the electric potential difference (MIV_L) and the sum of the same four constituents of the water transport, for the same time period. The best-fit line, in Fig. 9, was obtained by least-square method. The correlation between the two time-series allows an estimation of a water transport of 720 $m^3\ s^{-1}$ for each 1 mV potential difference between the ends of the cable.

The excellent correlation (720 $m^3\ s^{-1}\ mV^{-1}$) found between both variables allows the calibration of the electrical cable. The MIV_L values are multiplied by the calibration factor in order to convert them in to water transport of lunar origin.

Amplitude and phase lag for lunar origin tidal constituents for water transports both numerically computed and determined from the MIV_L (with the errors of the LSF for a significance level of 95 per cent), are plotted in Fig. 10(a). The adjustment between both series as regard amplitudes and phases is very good, and small differences between them are included in error bar. As an example of good adjustment of both series, the sums of the lunar constituents for water transports (both numerically computed and determined from the MIV_L) are compared in Fig. 10(b), including a zoom for a period of

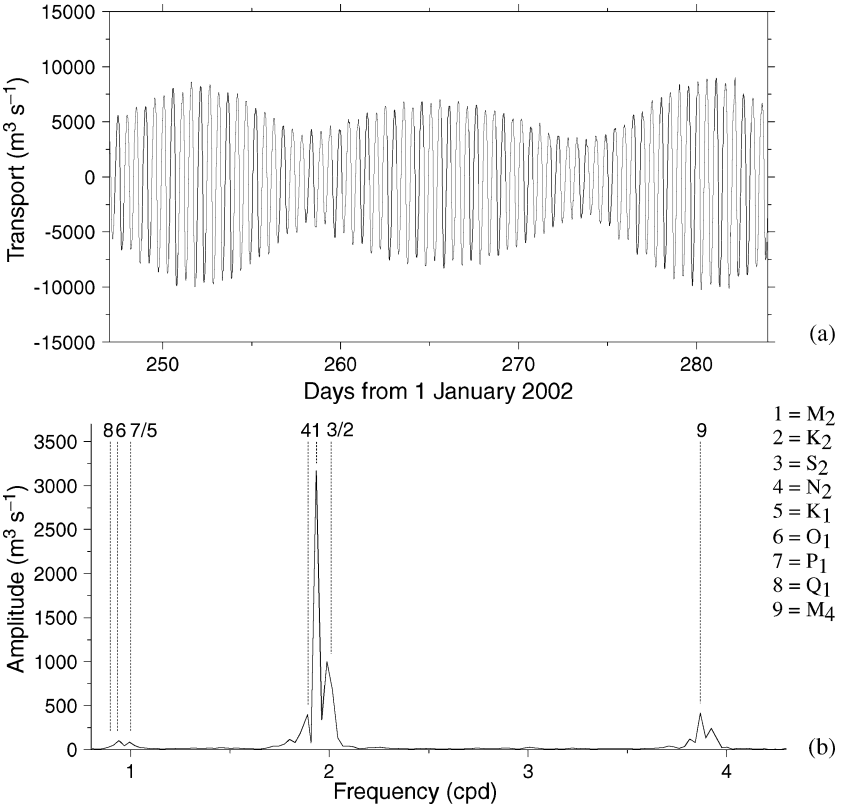

Figure 7. Water transport computed by the hydrodynamic numerical model (a) and its amplitude spectrum (b).

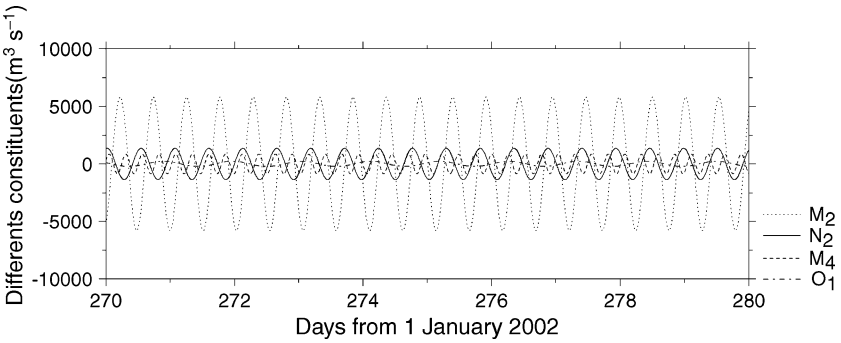

Figure 8. Harmonics of water transport with lunar origin, results of least-square analysis of water transport calculated using a 2-D model.

four tidal cycles, in order to better observe the adjustment resulting from the calibration.

These results show that the obtained calibration coefficient is well defined throughout the time-series. This coefficient could be used not only for tidal constituent, but also for longer period fluctuations.

To first order, the MIV (ΔV) is directly proportional to the conductivity-weighted vertical average of the flow velocity ($v*$). It scales linearly with the distance between electrodes (L) and the strength of the geomagnetic field component (B_z) perpendicular to both flow and electrical field, e.g. Sanford (1971), that is:

$$\Delta V = L\, B_z\, v^*, \tag{6}$$

where

$$v^* = \int_{-h}^{0} \sigma v\, dz \Big/ \int_{-h_s}^{0} \sigma\, dz,$$

h is the water depth and the integral in the denominator represents the sea water and sediments conductance down to a depth h_s where no electric current flows. For a non-stratified water, as in this case, v^* becomes: $v^*=\underline{v}/\lambda$, where $\lambda = 1 + S_s/S_w$. S_w and S_s are, respectively, the conductances of sea-water layer and the sediments layer below, and $\underline{v}$ is the mean velocity. The induced voltage should be proportional to the average transport ($t = \underline{v}\, Lh$):

$$t/\Delta V = h\lambda/B_z. \tag{7}$$

Considering $B_z = 36245$ nT (Preliminary Geomagnetic Bulletin 2002) and a 16.2 m depth (on average) for the channel, an estimation of $\lambda = 1.6$ is made. Under these conditions, taking $t/\Delta V$ as 720 m^3 s^{-1} mV^{-1}, the sediments conductance is about 33 S. The oceanic sediment layer may have an average conductivity of approximately half the conductivity of the sea water (Filloux 1987). Taking this value as a reference, a sediment layer of about 20 m

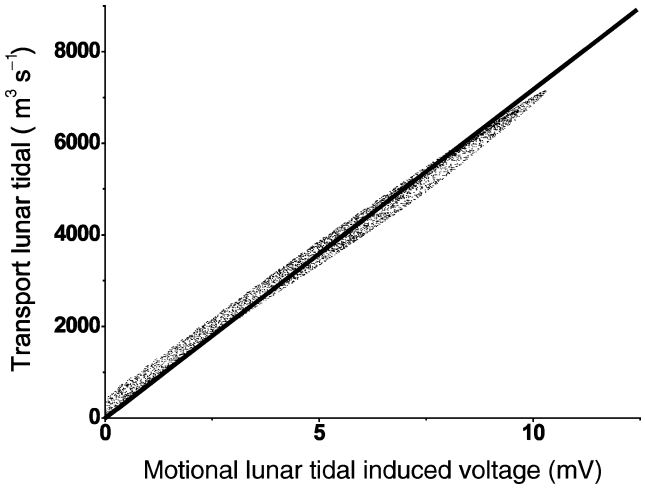

Figure 9. Calibration between motional field due to moon constituents of tides and the correspondent water transport. The regression line between both variables is also represented.

is estimated. There is little available information about the sediment layer at Barra. A seismic reflection profile which ends close to Barra location, shows the sedimentary cover exceeding 15 m (L.M. Pinheiro and H.G. Duarte, personal communication), which is not in disagreement with this estimation. However this profile was not made in the framework of this study, and its main goal was not the characterization of the sedimentary layer. Our results should, therefore, be compared with future geophysical studies in this area.

4 CONCLUSIONS

A value of 720 $m^3\ s^{-1}\ mV^{-1}$ was estimated for the coefficient relating voltage and water transport at Barra, that is, a transport of 720 $m^3\ s^{-1}$ is associated to each potential difference of 1 mV between the ends of the cable.

The data analysis reveals that measuring the differences of electrical potential across the channel can provide an accurate estimate of the water transport (by tidal and residual flows) through Barra channel. The possibility of using MIV methods to estimate flow transport on a short scale (about half of km) corresponding to

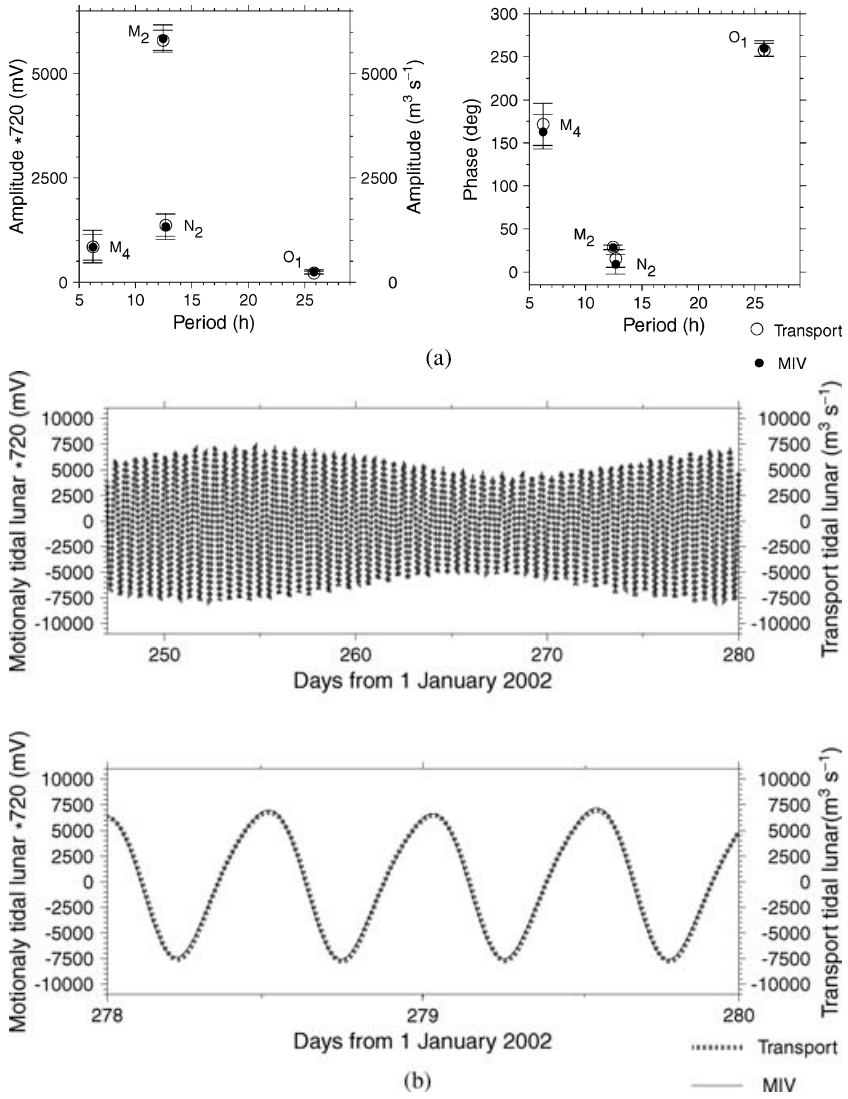

Figure 10. Lunar tidal constituents of the water transport determined by the numerical model and from the MIV_L, results of LSF approximation of the data with 95 per cent confidence interval. (a) Amplitude and phase, (b) Sums of lunar constituents.

estuarine systems, provides an important advantage over traditional oceanographic methods (classical currentmeter, Acoustic Doppler Currentmer Profiler, ADCP, etc.). In this kind of environment the use of traditional methodologies is clearly limited in cost and in time, due to batteries and memory limitations, as well as to the very fast growth of algae that will make difficult the proper functioning of the instruments. Furthermore, concerning the water flow is usually determined from discrete measurements while when using ADCP's there are shadow areas close to both the bottom and to the surface, and therefore the obtained results are only approximate values. The MIV methods present low cost for accurate long-term monitoring of integral water transport.

The main flows at the Barra channel have tidal origin and represent a key process in the water renewal at Ria de Aveiro lagoon. A quantitative analysis should be performed in order to obtain the residual flows. These residual weaker flows originate by sub-tidal currents variability, and are relevant in the study of the interchange mechanisms between the lagoon and the ocean. Residual flows analysis could be used for studying such phenomena as seasonal variations caused by river run-off, wind-forced currents, etc.

ACKNOWLEDGMENTS

This study was developed in the scope of the project PROTEU (PDCTM/MAR/15275/1999). Financial support was allocated by FCT under the Support Community Framework III, Operational Programme Science, Technology and Innovation. One of the authors MRN was also funded by a grant of the FCT (PRAXIS SFRH/BPD/10256/2002).

The authors would like to thank the Administration of the Port of Aveiro for the cession of the data of the tide gauge, and Irmãos Cavaco and Xavi-Sub for the aid in the installation of the cable. Thanks to the Area Militar de S. Jacinto are also due.

REFERENCES

Chave, A.D., Luther, D.S., Lanzerotti, L.J. & Medford, L.V., 1992. Geoelectric field measurements on a planetary scale: oceanographic and geophysical applications, *Geophys. Res. Lett.,* **19**(13), 1411–1414.

Dias, J.M., 2001. Contribution to the Study of the Ria de Aveiro Hydrodynamics, *PhD thesis,* Univ. de Aveiro, Portugal.

Dias, J.M., Lopes, J.F. & Dekeyser, I., 1999. Hydrological characterisation of Ria de Aveiro, Portugal, in early Summer, *Oceanologica Acta,* **22**(5), 473–480.

Dias, J.M., Lopes, J.F. & Dekeyser, I., 2003. A numerical model system application to the study of the transport properties in Ria de Aveiro lagoon, *Ocean Dynamics,* **53,** 220–231.

Dias, J.M. & Lopes, J.F., Implementation and Assessment of Hydrodynamic, Salt and Heat Transport Models: The Case of Ria de Aveiro Lagoon (Portugal), *Environmental Modelling & Software,* **21,** 1–15, doi:10.1016/j.envsoft.2004.09.002/.

Filloux, J.H., 1987. Instrumentation and experimental methods for oceanic studies, *New Volumes in Geomagnetism*; 1, Academic, New-York, 143–246.

Fristedt, T., Sigray, P., Lundberg, P. & Crona, L., 2002. Salt-wedge observations in Oresund by direct measurement of the motionally induced voltage, *Continental Shelf Research,* **22,** 2513–2524.

Flosadottir, A.H. & Taire, K., 1997. Observations of Ocean Currents Using Submarine Cables, *Proceedings of International Workshop on Scientific Use of Submarine Cables,* 10–15.

Harvey, R.R., Larsen, J.C. & Montaner, R., 1977. Electric field recording of tidal currents in the Strait of Magellan, *J. geophys. Res.,* **82,** 3472–3476.

Larsen, J.C., 1985. Florida Current volume transport from voltage measurements, *Science,* **227,** 292–311.

Larsen, J.C., 1992. Transport and heat flux of the Florida Current at 27 N derived from cross-stream voltages and profiling data: Theory and observations, *Phil. Trans. R. Soc. Lond.,* A, **338,** 169–236.

Leendertse, J.J., 1987. *Aspects of SIMSYS2D, a system for two-dimensional flow computation*. Report R-3572 USGS. New York, USA: The Rand Corporation.

Leendertse, J.J. & Gritton, E.C., 1971. *A Water–Quality Simulation Model for Well–Mixed Estuaries and Coastal Seas: Volume II, Computation Procedures*. Memorandum R-708-NYC. New York, USA: The Rand Corporation.

Monteiro Santos, F.A., Soares, A., Trindade, L., Nolasco, R., Rodrigues, H. & ISO3D team, 2002. Voltage measurements over the CAM-1 submarine cable between Madeira Island and Portugal mainland, *Earth Planets Space,* **54,** 393–398.

Palshin, N.A., Vanyan, L.L., Yegorov, I.V. & Lebedev, K.V., 1999. Electric field induced by the global ocean circulation, *Phys. Solid Earth,* **35**(12), 1028–1035.

Palshin, N.A., Vanyan, L.L., Medzhitov, R.D., Shapiro, G.I., Evdoshenko, M.A., Utada, H., Shimizu, H. & Tanaka, Y., 2001. Use of the Nakhodka-Naoetsu submarine cable for studying the temporal variability of integral water transport in the Sea of Japan, *Oceanolgy,* **41**(3), 447–457.

Palshin, N.A., Vanyan, L.L., Poray-Koshits, A.M., Matyushenko, V.A., Kaikkonen, P. & Tiikkainen, J., 2002. Measurements of motionally induced voltage in the coastal zone of the Throat of the White Sea, *Earth Planets Space,* **54,** 433–441.

Pawlowicz, R., Beardsley, B. & Lentz, S., 2002. Classical tidal harmonic analysis including error estimates in Matlab using T_Tide, *Computers &Geosciences,* **28,** 929–939.

Preliminary Geomagnetic Bulletin, 2002. *Observatorio Magnético do Instituto Geofisico da Universidade de Coimbra*, Ns. 463 to 467.

Sanford T.B., 1971. Motionally Induced Electric and Magnetic Fields in the Sea, *J. geophys. Res.,* **76,** 3476–3492.